Supplement of Atmos. Chem. Phys., 15, 6827–6849, 2015
http://www.atmos-chem-phys.net/15/6827/2015/
doi:10.5194/acp-15-6827-2015-supplement

Supplement of

Seasonal variability of atmospheric nitrogen oxides and non-methane hydrocarbons at the GEOSummit station, Greenland

L. J. Kramer et al.

Correspondence to: L. J. Kramer (lkramer@mtu.edu)

1 Calibration procedures and uncertainty estimates for the nitrogen oxides instrument

The sensitivity of the instrument to NO was determined via the standard addition of NO, and ranged from 2.3 to 5.9 counts s^{-1} per pmol mol^{-1} (cps ppt^{-1}) , with a median value of 2.7 cps ppt^{-1}. To ensure that the instrument operated optimally during periods with limited supervision, a number of additional calibrations were performed to determine the zeroing efficiency, the response of the NO_2 and NO_y converters, and artifact corrections. The NO_2 and NO_y converters were both calibrated for the conversion of NO_2 to NO through the standard addition of NO_2 at the inlets. NO_2 was generated via gas phase titration of the NO standard with O_3. The NO_2 conversion efficiency remained stable at 52 ± 5 (mean ± 2σ) during the 2 years of measurements. Conversion efficiencies for NO_2 in the NO_y converter were typically above 96% (median 99%). Calibration mole fractions for n-propyl nitrate (NPN, 4.4 to 220 nmol mol^{-1}) and nitric acid (HNO_3, 1.4 to 9.7 nmol mol^{-1}) were determined every 3 days from standard addition of each species with the NO_y converter heated to 300°C (regular operating temperature) and 500°C. At 500°C the conversion efficiency of the NO_y species is expected to be > 95% (Bollinger et al. 1983; Fahey et al. 1985). The conversion efficiencies were calculated to be typically > 80% (median 95%) for NPN and > 85% (median ~101%) for HNO_3. The potential interference due to conversion of non-NO_y species was estimated using the standard addition of acetonitrile (CH_3CN), which is typically observed in biomass-burning plumes (de Gouw et al. 2004; Holzinger et al. 2005). Measurements of CH_3CN were obtained twice daily during the regular calibrations and referenced to the calibration standard from two permeation devices used during the measurement period, which were determined using the manufacturer's reported permeation rate (21 and 246 nmol mol^{-1}). The CH_3CN conversion was always below 4%, with a median value of 0.9%, confirming that CH_3CN did not significantly contribute to the total NO_y measurements. The NO_y inlet is based on the same design used at Pico, which uses a filter to exclude aerosols with diameters greater than 10μm (Val Martin et al. 2008). Smaller aerosols were able to be sampled, however, the gold-catalyzed converter does not efficiently convert most fine aerosols except NH_4NO_3 (Miyazaki 2005).

At low mole fractions uncertainty in the artifact correction is important. The artifact for NO_y was determined once a week, while artifacts for NO and NO_2 were performed twice weekly. Artifact values for NO and NO_y were constant during uninterrupted periods of measurements. Small changes in the NO and NO_y artifact occurred after the instrument was switched off for prolonged periods or after instrument maintenance was performed. The artifact corrections applied to the data ranged between -5 to 1.5 pmol mol^{-1} (NO) and 2 to 15 pmol mol^{-1} (NO_y). Time-varying artifacts were determined for NO_2 as the artifact decreased after time due to a reduction in cell contaminants within the converter. The NO_2 artifact applied to the data varied between 14 to 30 pmol mol^{-1} over the two years of measurements. Uncertainty in the artifact corrections were estimated to be ± 2 pmol mol^{-1} for NO, ± 5 pmol mol^{-1} for NO_2, and ± 5 pmol mol^{-1} for NO_y.

The accuracy in the measurements is also dependent on the uncertainty in the flow rates measured by the sample (1%) and calibration (5%) mass flow controllers (MFCs) and the NO standard calibration gas mole fraction. The NO standards are quoted with an accuracy of 2% traceable to primary standards by the manufacturers. The NO calibration cylinders were also compared to a NIST standard (NIST standard reference 2628a, 10 ppmv) in the field. However, the results from the intercomparisons show a consistent positive bias with mole fractions outside the specified uncertainties. Analysis of the intercomparison tests suggests that the instrument calibration lines did not fully stabilize when switching from the high mole fraction of the NIST standard to the working standard. Therefore, greater confidence is with the manufactures stated mole fractions than those obtained from the intercomparisons with the NIST standard. The accuracy in the NO and NO_2 measurements from the MFCs and calibration standard is estimated to be 6% from error propagation. For NO_y, the accuracy also depends on the efficiency of the NO_y converter and biases resulting in the conversion of non-NO_y species, as discussed above. Based on typical values of NO_y at Summit, the negative bias resulting from the non-conversion of NO_y species is estimated to be ~10% if we take the lower limits of the conversion efficiencies. Typically the negative bias will be ~2% based on median conversion efficiencies observed during the measurement period. The positive bias resulting from conversion of CH_3CN in the converter would be greatest when observing biomass burning plumes. During ARCTAS-B high CO levels (>160 ppbv) had a mean CH_3CN level of 520 pmol mol^{-1}, which were attributed to biomass burning plumes, and those with CO levels from 120 - 160 ppbv, had CH_3CN levels of 200 pmol mol^{-1} and were mainly from anthropogenic pollution (Liang et al., 2011). Using these values, the maximum interference of CH_3CN at NO_y levels of 200 pmol mol^{-1} (based on a conversion efficieny of 4% would be ~10% in biomass-burning plumes and ~4% in anthropogenic plumes. Typically this would be ≤ 2% when considering the median conversion efficiency of CH_3CN of 0.9%.

Through the propagation of errors the NO_y measurement accuracy is estimated to be ~12% in the worst case senario and typically ~6%. Total uncertainty in the measurements is determined from the measurement accuracy, artifact and precision of the data. The precision of the data is related to the photon-counting noise of the detector and is also used to estimate the limit of detection of the instrument. For NO, NO_2 and NO_y the precision is estimated as the 2σ standard error of the 30 s averages (20 s for NO_y) with median values of 4.6 pmol mol^{-1} (NO), 8.4 pmol mol^{-1} (NO_2) and 6.4 pmol mol^{-1} (NO_y). The data were further averaged to 30 min averages, giving a median 2σ precision of 2.7 pmol mol^{-1} for NO, 5.0 pmol mol^{-1} for NO_2, 5.7 pmol mol^{-1} for NO_x, and 3.8 pmol mol^{-1} for NO_y. Ninety nine percent of the data have a 2σ precision of less than 3.7 pmol mol^{-1}, 6.5 pmol mol^{-1}, 7.5 pmol mol^{-1} and 5.2 pmol mol^{-1} for NO, NO_2, NO_x, and NO_y respectively.

2. Supplementary Figures

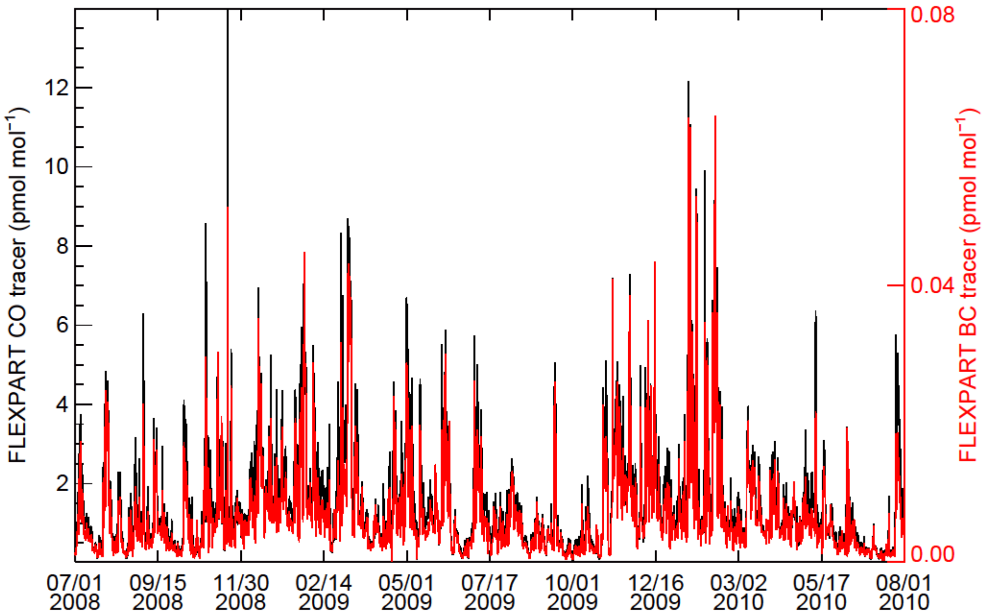

Figure S1. Time series of the FLEXPART CO tracer (black) and the FLEXPART BC tracer (red) at Summit for July 2008 to July 2010.

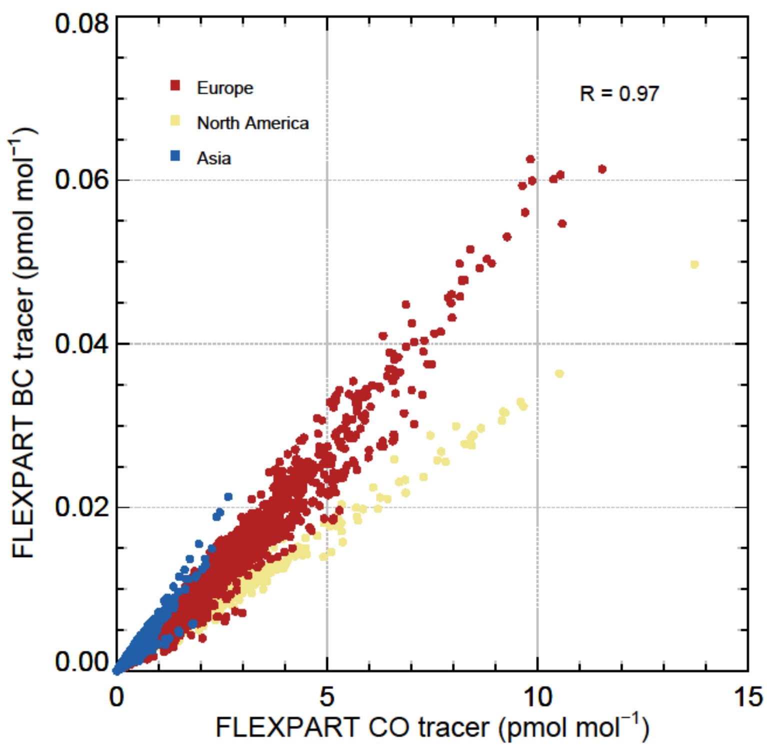

Figure S2. Correlation of FLEXPART CO tracer and the FLEXPART BC tracer at Summit for July 2008 – July 2010. Colors represent the source regions for each tracer as shown in the legend. The Pearson's correlation coefficient (R) for all the data is shown in the upper right corner of the plot.

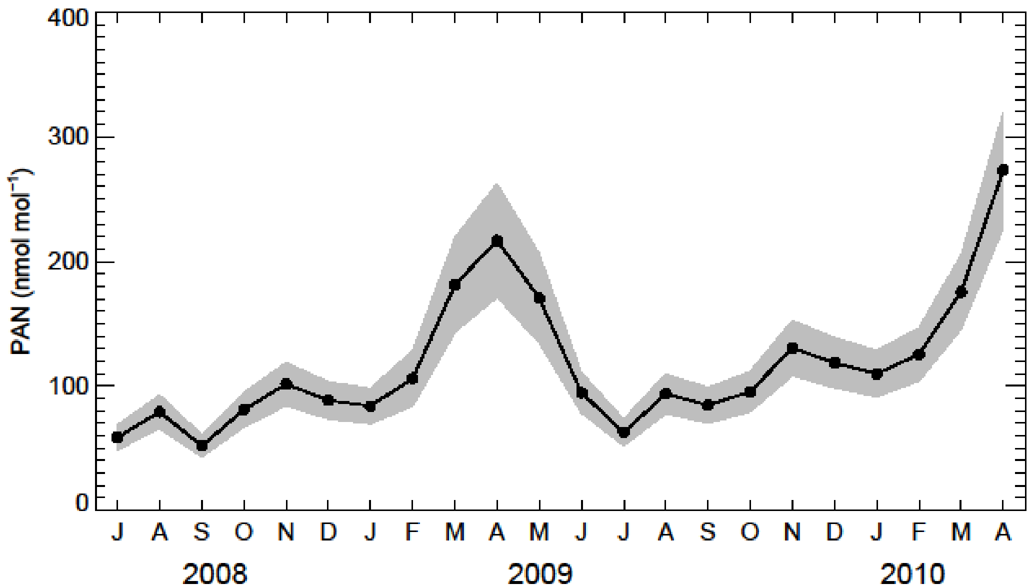

Figure S3: Monthly mean PAN mole fractions measured at Summit. Shaded regions represent the measurement uncertainty of the data.

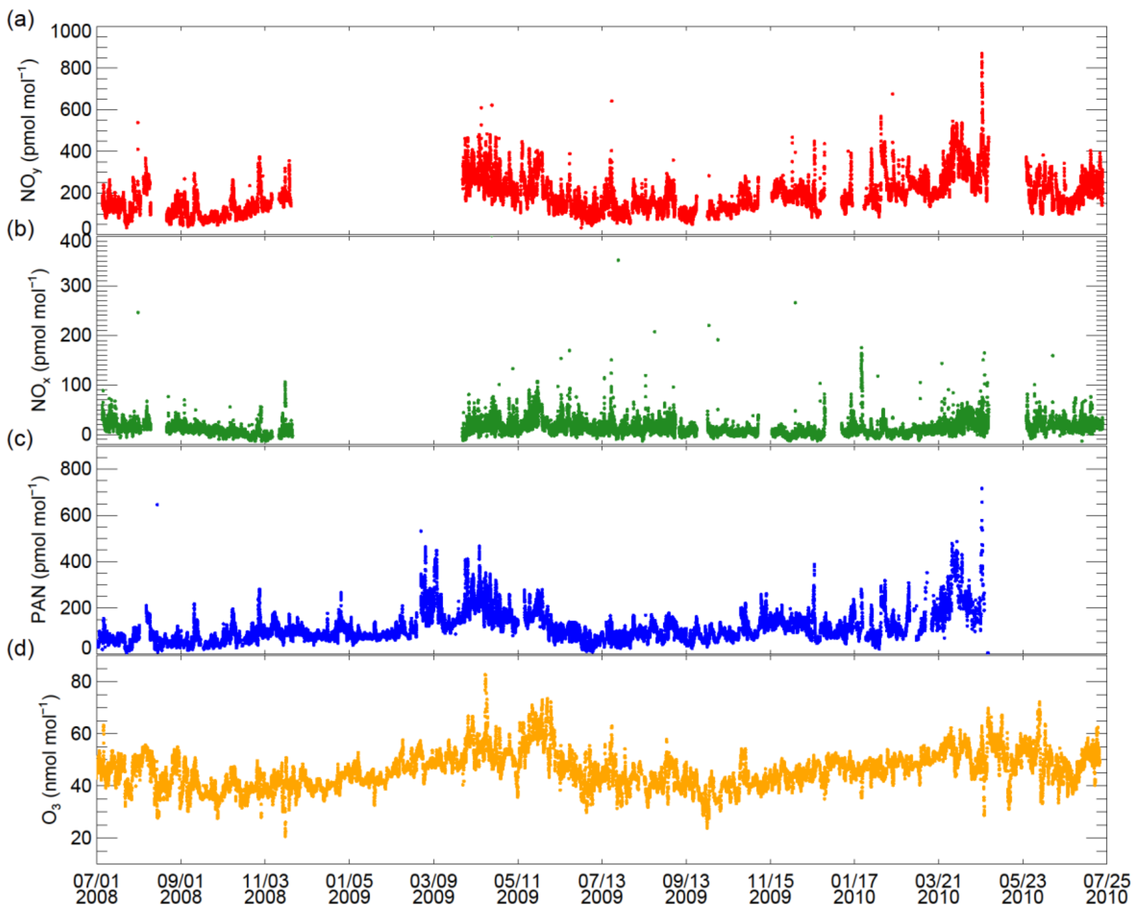

Figure S4: 30 min averaged mole fractions of a) NO_y, b) NO_x, c) PAN and 1 hour averages of d) O_3, for the period 1 July 2008 to 25 July 2010, measured at Summit, Greenland.

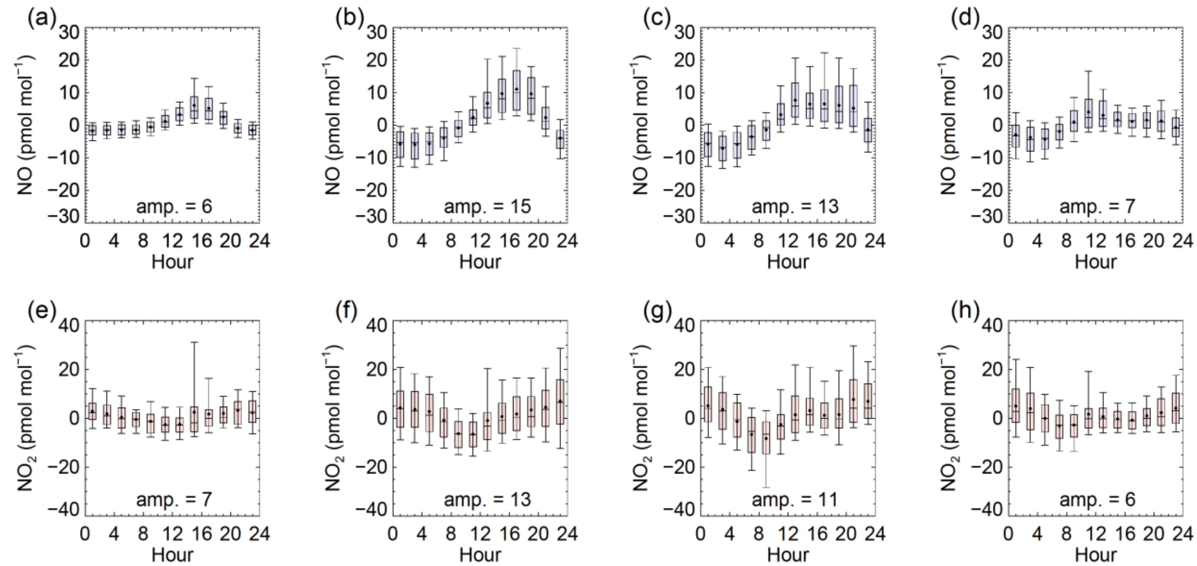

Figure S5: Average diurnal cycle of ambient NO **(a, b, c, d)** and NO_2 **(e, f, g, h)** measured at Summit for the months March (1st column), April (2nd column), May (3rd column) and, June (4th column) 2008 2010. Median ambient levels observed each day were subtracted, to remove any impact from day to day variability. The median and mean of the data are represented by a horizontal line, and filled black circle, respectively; the box indicates the middle 67% of the data; and the vertical whiskers indicate the 5th and 95th percentile of all the data. Times are shown as local time (UTC).The amplitude of the diurnal cycle (given as the difference between the lowest and highest 2 hour median values, in pmol mol^{-1}) is noted on each subplot.

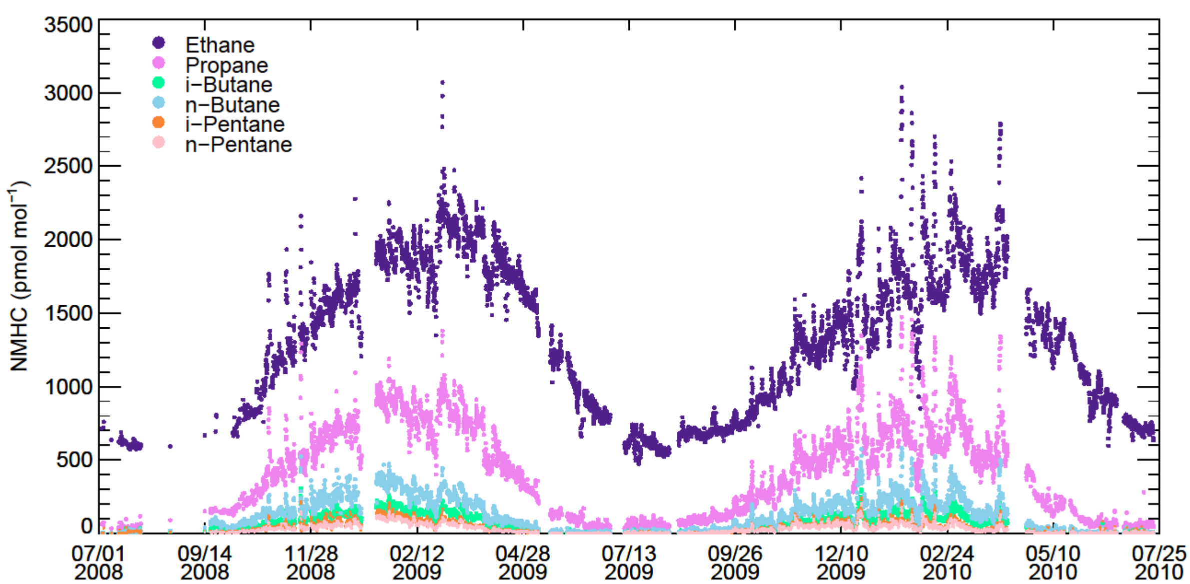

Figure S6: Times series of NMHC mole fractions measured at Summit during for the period 1 July 2008 to 25 July 2010.

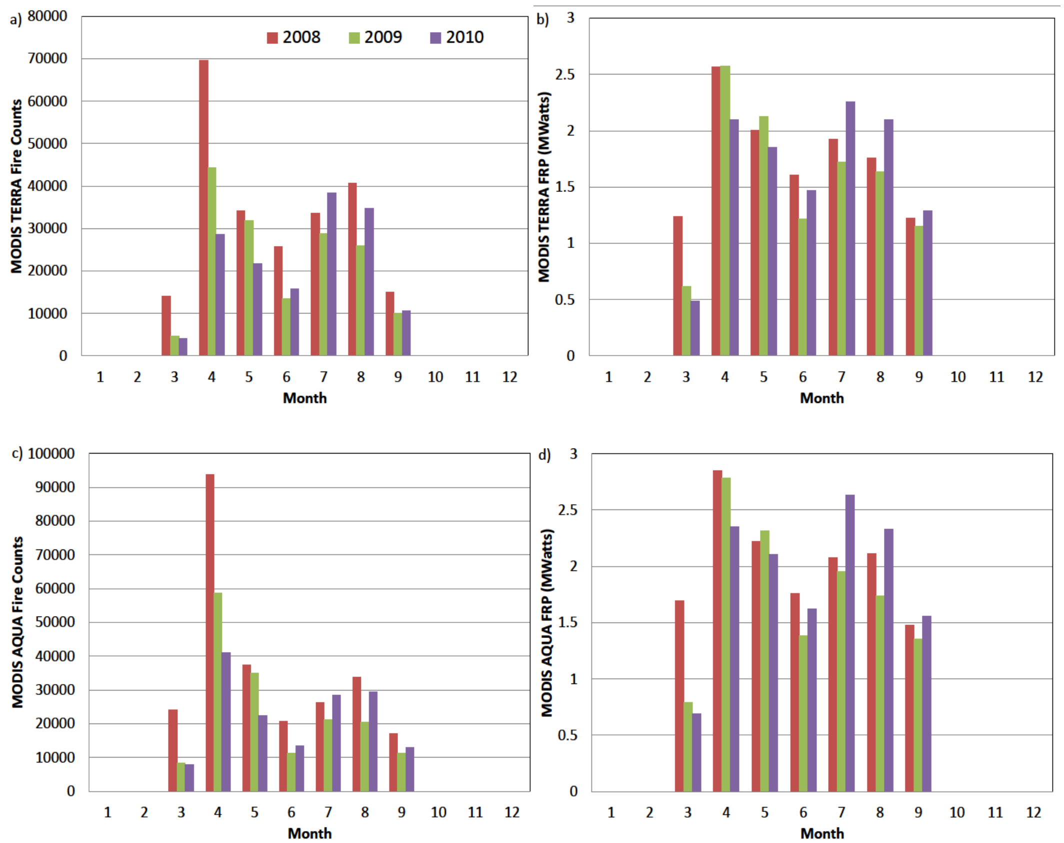

Figure S7. Top Panel: a) Total monthly overpass and cloud corrected fire pixel count and b) Fire Radiative Power (FRP) for Terra. Bottom Panel: c) and d) are the same for the Aqua satellite. All values are averaged over the zonal region 40-75 N. Data downloaded from the University of Maryland ftp server (ftp://fuoco.geog.umd.edu).

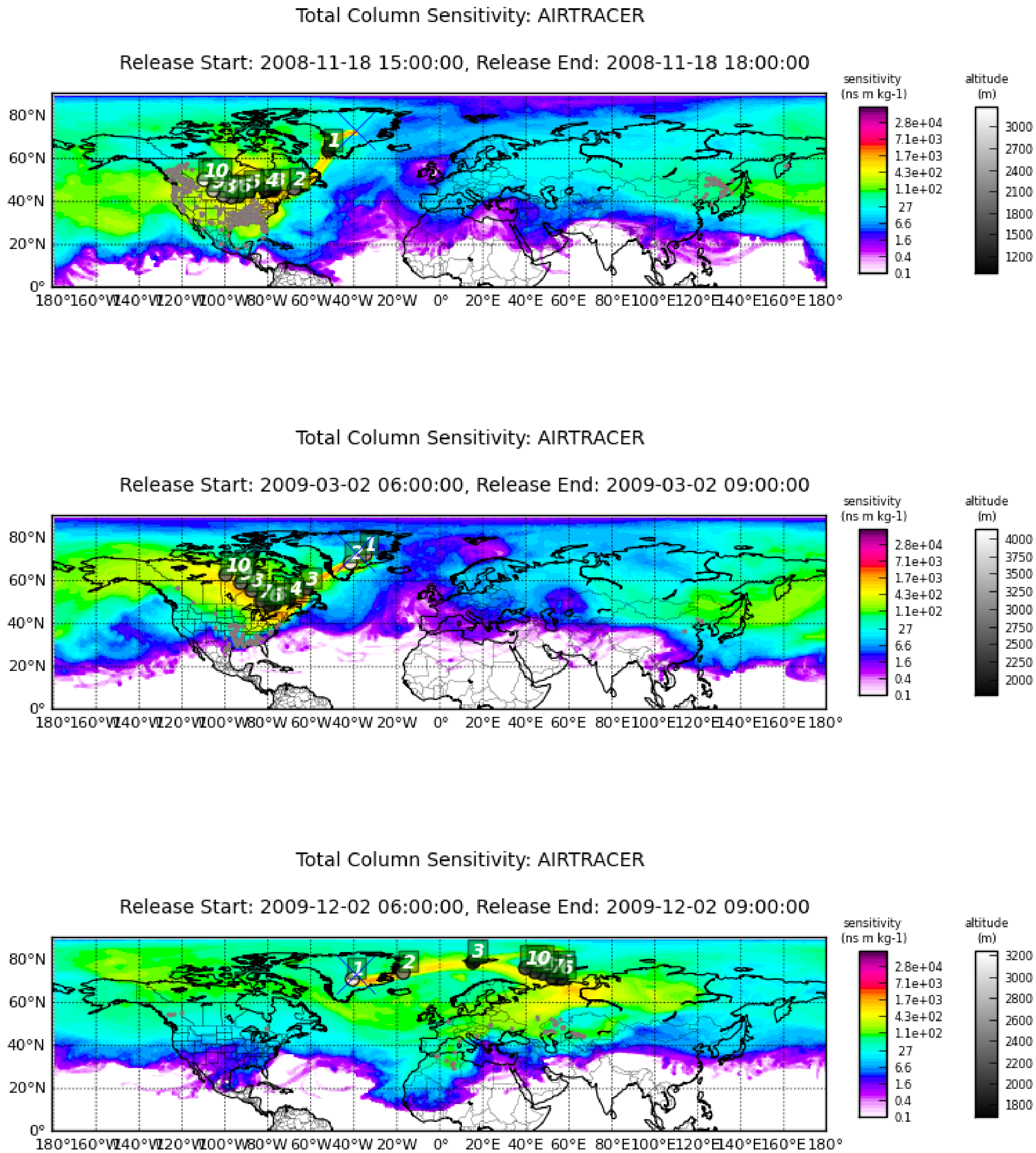

Figure S8: FLEXPART simulated total column sensitivity (ns m kg^{-1}) for retroplumes that are representative of the air mass transport during five anthropogenic events (#16, 34, 60, 17, and 28) with negative mean ΔO_3 values (ranging from -6.7 to -1 nmol mol^{-1}). The altitude circles represent the centroid location of the particles in the model domain N days back from the measurement date, where N is the number shown next to the shaded circles (up to 10 days are shown on the plots). The shading represents the altitude of the centroid location, given by the gray-scale bar.

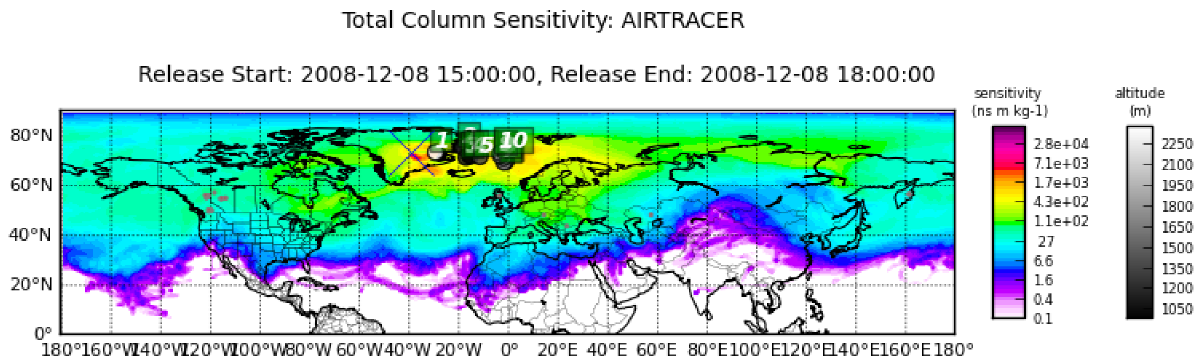

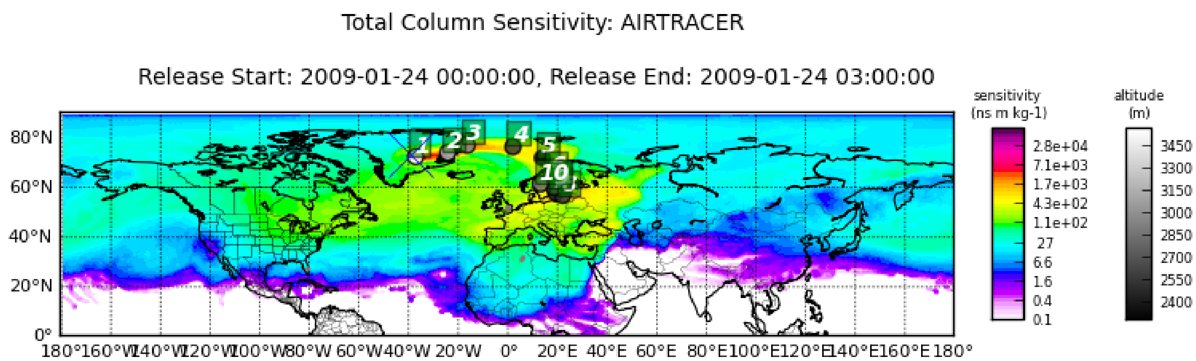

Figure S8: Continued from previous page.

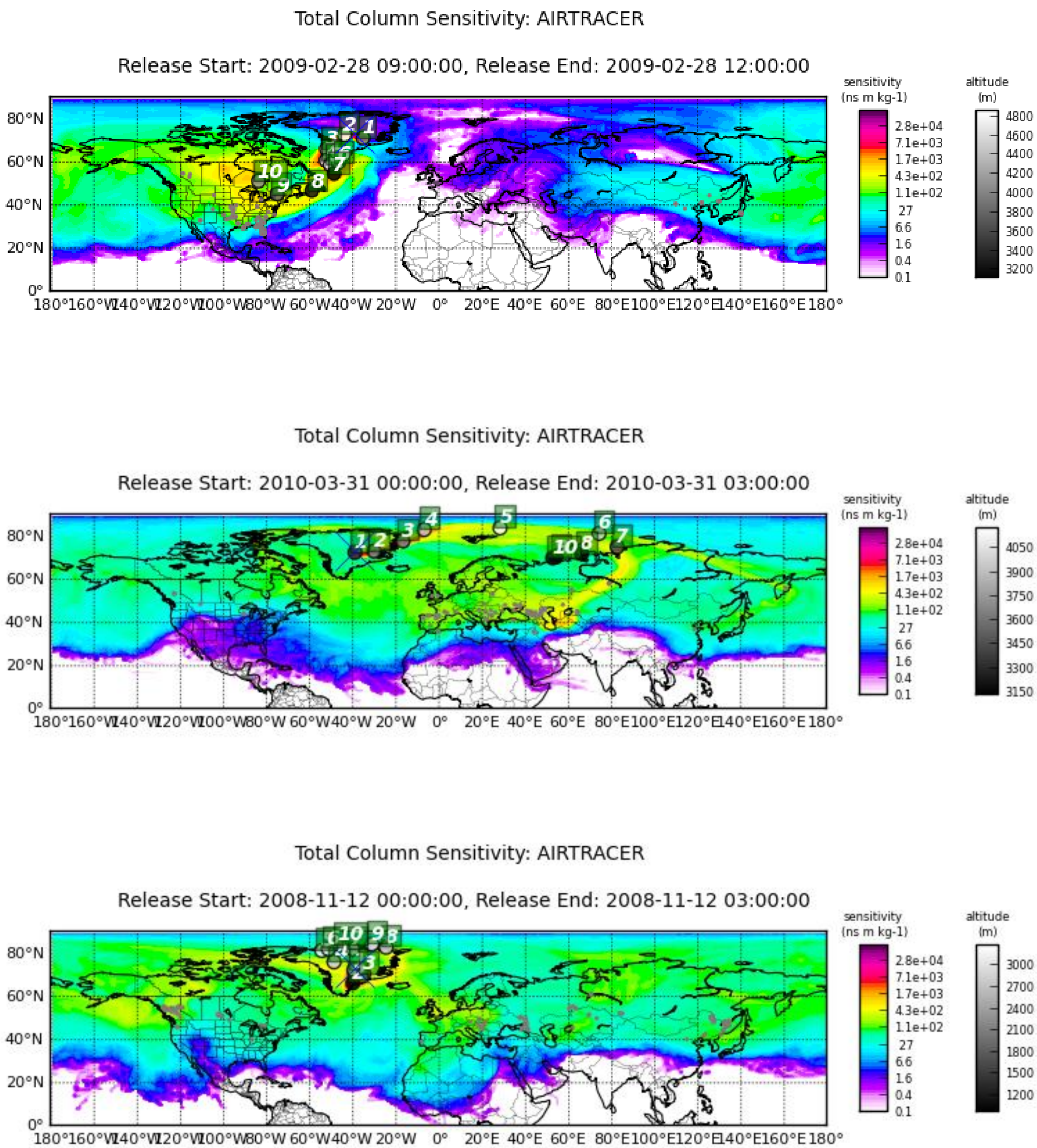

Figure S9: FLEXPART simulated total column sensitivity (ns m kg^{-1}) for retroplumes that are representative of the air mass transport during the six anthropogenic events (#33, 80, 14, 32, 64, and 13) over winter with the highest mean ΔO_3 values (ranging from 4.3 to 7.6 nmol mol^{-1}). The altitude circles represent the centroid location of the particles in the model domain N days back from the measurement date, where N is the number shown next to the shaded circles (up to 10 days are shown on the plots). The shading represents the altitude of the centroid location, given by the gray-scale bar.

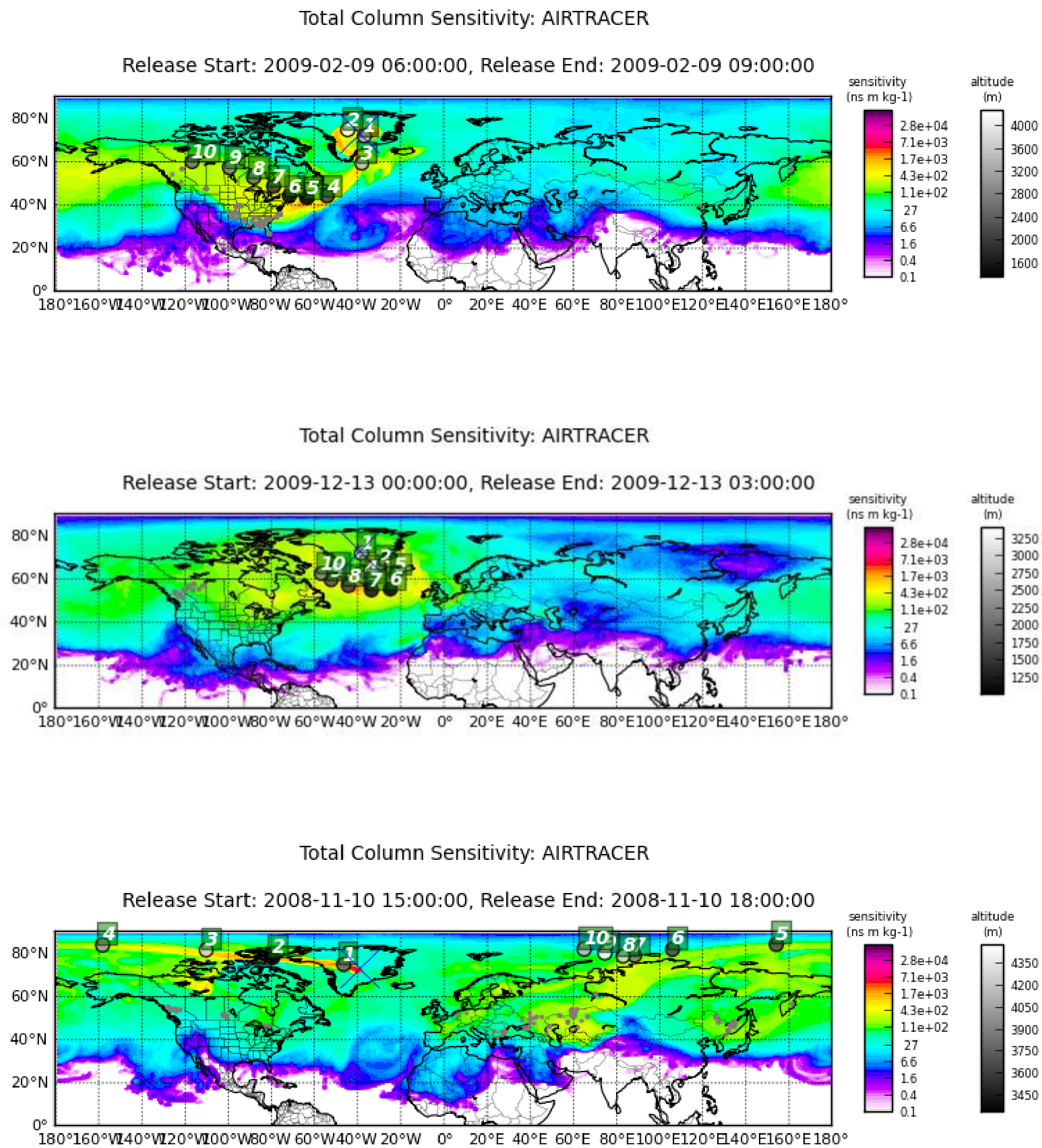

Figure S9: Continued from previous page.

3. Supplementary Tables

Table S1: Combustion efficiency, emission factor, and fuel load factors used to estimate the BC fire emissions in FLEXPART.

Category:	Forest (NOAH LSM 1-5)	Shrubland (NOAH LSM 6-9)	Grassland (NOAH LSM 10)	Crops (NOAH LSM 12)	Urban / Bare (NOAH LSM 11)
Fuel load	14	4	1	0.5	0.1
Combustion Efficiency	0.4	0.5	0.9	0.9	0.9
Emission Factor	0.107	0.080	0.065	0.092	0.070

Table S2: Mean enhancements in trace gases measured at Summit during anthropogenic events.

Event #	Start Date	Length (hrs)	BC_{anthro} peak (pmol mol^{-1})	ΔO_3 (pmol mol^{-1})	ΔNO_x (pmol mol^{-1})	ΔNO_y (pmol mol^{-1})	ΔPAN (pmol mol^{-1})	ΔC_2H_6 (pmol mol^{-1})	Plume age (days)
1	7/4/2008	12	0.012	4.6	-	-	30.9	-	8
2	7/5/2008	21	0.017	8.6	21.1	81.8	63.5	-	9
3	7/28/2008	18	0.025	6.0	10.0	98.7	70.0	0.0	9
4	7/29/2008	66	0.023	8.2	13.2	84.0	59.9	8.2	10
5	8/2/2008	18	0.011	10.6	0.2	61.7	-	-	12
6	9/1/2008	27	0.023	1.1	6.7	29.8	24.7	-	7
7	9/12/2008	51	0.016	6.4	11.7	89.5	59.7	0.0	9
8	10/9/2008	54	0.017	8.0	12.0	108	95.3	56.3	10
9	10/12/2008	18	0.011	6.0	2.9	37.6	59.8	60.0	11
10	10/29/2008	39	0.030	3.6	12.5	193	146	757	10
11	10/31/2008	12	0.014	-1.5	44.9	138	60.6	500	9
12	11/8/2008	27	0.030	-0.4	-	-	43.4	0.0	9
13	11/10/2008	18	0.012	4.3	-	-	65.6	531	14
14	11/12/2008	18	0.021	5.7	-	-	20.4	131	11
15	11/13/2008	15	0.017	3.8	2.8	40.7	2.9	117	13
16	11/18/2008	18	0.051	-6.7	60.3	69.2	-	-	9
17	12/8/2008	18	0.012	-1.9	-	-	1.9	177	13
18	12/9/2008	27	0.012	0.2	-	-	-7.3	137	11
19	12/14/2008	42	0.016	0.9	-	-	3.9	99.9	13
20	12/16/2008	117	0.035	-0.3	-	-	11.5	183	12
21	12/23/2008	21	0.011	2.0	-	-	9.6	106	15
22	12/26/2008	12	0.018	0.2	-	-	54.3	223	14
23	12/27/2008	33	0.021	2.7	-	-	57.9	48.3	10

24	1/6/2009	54	0.020	3.8	-	-	10.6	-	12
25	1/9/2009	51	0.013	3.8	-	-	-1.1	-	13
26	1/18/2009	12	0.011	0.2	-	-	9.0	34.0	13
27	1/19/2009	45	0.021	0.4	-	-	9.6	54.3	8
28	1/23/2009	63	0.025	-1.0	-	-	26.5	111	12
29	1/26/2009	69	0.045	1.4	-	-	3.9	103	10
30	1/31/2009	12	0.009	-0.1	-	-	12.2	207	15
31	2/4/2009	48	0.029	-0.2	-	-	9.6	126	11
32	2/9/2009	18	0.012	4.6	-	-	48.5	275	10
33	2/27/2009	30	0.015	7.6	-	-	165	278	13
34	3/1/2009	30	0.032	-3.7	-	-	154	420	8
35	3/4/2009	75	0.022	1.1	-	-	53.1	112	12
36	3/7/2009	114	0.043	2.1	-	-	153	111	10
37	3/14/2009	72	0.020	-0.2	-	-	16.9	145	14
38	4/16/2009	12	0.011	6.4	8.6	108	107	81.0	13
39	4/19/2009	63	0.024	3.7	19.4	89.7	51.1	68.8	10
40	4/30/2009	96	0.029	1.5	-1.4	37.8	21.5	332	9
41	5/5/2009	33	0.020	2.5	7.2	69.5	47.9	386	10
42	5/6/2009	24	0.012	-1.3	10.4	-9.4	-18.1	429	12
43	5/13/2009	30	0.020	3.0	7.2	137	-	-	7
44	5/15/2009	12	0.010	11.4	16.1	96.8	-	-	10
45	5/27/2009	21	0.014	8.8	-	-	58.2	-	15
46	6/4/2009	90	0.030	15.0	1.3	43.5	31.4	147	10
47	6/9/2009	30	0.020	7.7	9.2	32.7	29.8	-37.6	13
48	7/2/2009	24	0.026	0.7	8.1	-9.4	-6.0	-	10
49	7/5/2009	60	0.019	2.3	9.0	21.7	-10.7	-	12
50	7/8/2009	27	0.018	6.6	-4.0	22.4	27.3	17.0	12
51	8/5/2009	57	0.013	5.9	9.0	63.8	43.2	-15.2	10
52	9/13/2009	18	0.026	7.5	3.4	1.4	-7.7	15.1	6
53	9/14/2009	27	0.020	6.4	5.2	1.6	-7.2	30.7	7
54	10/28/2009	102	0.023	3.9	9.0	53.6	20.4	296	12
55	11/6/2009	111	0.041	-0.5	29.8	85.3	55.3	88.7	11
56	11/11/2009	81	0.022	1.3	-	-	49.2	143	12
57	11/15/2009	36	0.016	2.5	6.6	47.6	51.1	74.9	14
58	11/17/2009	45	0.013	3.7	4.0	67.1	34.1	44.8	15
59	11/20/2009	87	0.039	3.2	10.9	85.9	56.5	113	13
60	12/1/2009	30	0.023	-2.1	1.7	63.5	27.1	39.1	12
61	12/6/2009	15	0.022	0.1	19.9	89.2	53.3	175	9
62	12/8/2009	42	0.035	-0.2	10.7	81.8	53.6	181	9
63	12/10/2009	63	0.026	2.0	4.4	67.1	45.3	142	10
64	12/13/2009	15	0.012	4.5	15.1	63.5	51.8	-46.8	9
65	12/14/2009	54	0.044	1.6	7.0	14.8	5.4	213	9
66	12/23/2009	39	0.011	-0.9	2.4	59.8	32.8	728	15

67	1/11/2010	18	0.017	1.8	1.2	33.9	17.6	233	10
68	1/14/2010	126	0.064	0.2	18.3	84.6	72.3	374	10
69	1/20/2010	27	0.020	0.0	9.5	-	21.6	401	10
70	1/22/2010	33	0.053	-6.0	87.7	-	125	1036	8
71	1/29/2010	27	0.035	-0.7	10.6	184	92.1	1119	10
72	1/31/2010	45	0.030	0.1	1.1	-8.8	-22.4	-120	11
73	2/2/2010	12	0.016	4.1	1.7	4.1	-1.6	-245	13
74	2/6/2010	105	0.065	-0.1	22.4	198	132	469	9
75	2/11/2010	45	0.023	3.6	4.5	16.9	12.7	199	11
76	2/14/2010	12	0.018	2.3	35.8	334	50.1	321	15
77	3/9/2010	87	0.021	2.8	5.3	70.0	57.8	217	10
78	3/14/2010	81	0.015	1.2	4.4	-17.2	38.5	3.4	12
79	3/20/2010	18	0.013	3.0	5.9	-1.7	51.2	-38.8	13
80	3/30/2010	18	0.013	5.9	-1.9	262	295	289	14
81	4/2/2010	33	0.012	-0.2	-2.7	184	175	1190	15
82	4/3/2010	24	0.015	2.5	14.6	173	181	716	14
83	4/7/2010	18	0.013	8.5	24.7	204	168	492	11
84	5/11/2010	15	0.022	-5.9	-	-	-	216	7
85	5/18/2010	51	0.014	4.1	-	-	-	-	12

References

Bollinger, Mark J, Robert E Sievers, David W Fahey, and Frederick C Fehsenfeld. 1983. “Conversion of Nitrogen Dioxide, Nitric Acid, and N-Propyl Nitrate to Nitric Oxide by Gold-Catalzed Reduction with Carbon Monoxide.” *Analytical Chemistry* 55: 1980–86.

Fahey, D. W., C. S. Eubank, G. Hubler, and F. C. Fehsenfeld. 1985. “Evaluation of a Catalytic Reduction Technique for the Measurement of Total Reactive Odd-Nitrogen NO_y in the Atmosphere.” *Atmospheric Chemistry.* 3: 435–68.

De Gouw, J. A., O. R. Cooper, C. Warneke, P. K. Hudson, F. C. Fehsenfeld, J. S. Holloway, G. Hubler, D. K. Nicks Jr., J. B. Nowak, D. D. Parrish, T. B. Ryerson, E. L. Atlas, S. G. Donnelly, S. M. Schauffler, V. Stroud, K. Johnson, G. R. Carmichael, and D. G. Streets. 2004. “Chemical Composition of Air Masses Transported from Asia to the U.S. West Coast during ITCT 2K2: Fossil Fuel Combustion versus Biomass-Burning Signatures.” *Journal of Geophysical Research* 109(D23S20).

Holzinger, R., J. Williams, G. Salisbury, T. Klüpfel, M. de Reus, M. Traub, P. J. Crutzen, and J. Lelieveld. 2005. “Oxygenated Compounds in Aged Biomass Burning Plumes over the Eastern Mediterranean: Evidence for Strong Secondary Production of Methanol and Acetone.” *Atmospheric Chemistry and Physics* 5(1): 39–46.

Liang, Q., Rodriguez, J. M., Douglass, A. R., Crawford, J. H., Olson, J. R., Apel, E., Bian, H., Blake, D. R., Brune, W., Chin, M., Colarco, P. R., da Silva, A., Diskin, G. S., Duncan, B. N., Huey, L. G., Knapp, D. J., Montzka, D. D., Nielsen, J. E., Pawson, S., Riemer, D. D., Weinheimer, A. J., and Wisthaler A. 2011. "Reactive nitrogen, ozone and ozone production in the Arctic troposphere and the impact of stratosphere-troposphere exchange." *Atmospheric Chemistry and Physics*. 11,13181–13199, doi:10.5194/acp-11-13181-2011.

Miyazaki, Y. 2005. “Contribution of Particulate Nitrate to Airborne Measurements of Total Reactive Nitrogen.” *Journal of Geophysical Research* 110(D15): D15304.

Val Martin, M., R. E. Honrath, R. C. Owen, and Q. B. Li. 2008. “Seasonal Variation of Nitrogen Oxides in the Central North Atlantic Lower Free Troposphere.” *Journal of Geophysical Research* 113(D17): D17307.